

LONDON
SCHOOL of
HYGIENE
& TROPICAL
MEDICINE



LSHTM Research Online

Wang, XS; Dytham, C; (2008) Full-length conference Paper at The 2nd York Doctoral Symposium on Computer Science and Electronics. [Conference or Workshop Item]
<https://researchonline.lshtm.ac.uk/id/eprint/1366915>

Downloaded from: <http://researchonline.lshtm.ac.uk/1366915/>

DOI:

Usage Guidelines:

Please refer to usage guidelines at <https://researchonline.lshtm.ac.uk/policies.html> or alternatively contact researchonline@lshtm.ac.uk.

Available under license: <http://creativecommons.org/licenses/by-nc-nd/2.5/>

<https://researchonline.lshtm.ac.uk>

A Hierarchical Metapopulation Model for Disease Dynamics Built on Population Movements of Both Patch-Coupling and Migration

Xiaosi Wang^{1,2} and Calvin Dytham²

¹ Department of Health Sciences, University of York, York YO10 5DD, United Kingdom

² Department of Biology, University of York, York YO10 5DD, United Kingdom

Abstract. In the past, frequent movements and migration were studied separately in metapopulation models. The levels that exist in a hierarchical metapopulation model were also limited to two and only recently increased to multiple levels. Moreover, a generalisable deterministic model was not available. Here we introduce a novel model incorporating both movement scenarios as well as a multiple-level structure. We describe the system in simple differential equation form. The simulations of different distributions of local contact rates for disease transmission suggest that local information is important for predicting disease dynamics. The comparison between the results from a solely migration-based multilevel model and the model discussed in this paper suggests that diseases with low transmission rates can spread rapidly and infect a large number of susceptible individuals in a short time if they appear in a population where frequent movements are dominant.

Keywords: multilevel system, patch-based system, disease modelling, epidemic, mathematical epidemiology

1 Introduction

It is now clear that understanding and prediction of the progress of disease requires consideration of the spatial arrangement of individuals and many recent computational models of disease spreading place a strong emphasis on the role of the spatial heterogeneity of human populations [1–3]. It is clear that the distribution of individuals within a population significantly affects the process of pathogen dispersal, but the exact operating functions linking transmission and spatial pattern are still unknown. However, even when using pathogen-related parameters that are invariant, e.g. a model where pathogen infectivity and virulence are kept constant throughout the simulations, the results generated by spatial models simulate the real epidemics very well [2, 4–6].

There are various ways to integrate spatial heterogeneity into models. One popular method is to build metapopulation models, where the population is divided into a network of smaller subpopulations on patches [2, 7, 8]. Individuals within each subpopulation are assumed to be well mixed. Metapopulation models allow explicit mathematical expressions and straightforward numerical solutions [9], and hence play an important role in mathematical epidemiology. Hierarchical metapopulation models are a special type of general metapopulation models [2, 10]. They consider

16 the hierarchy involved in human movements (i.e. that subpopulations have some non-random pat-
17 tern of connections) [11, 12] and simulations from these models show that disease spreading is
18 significantly influenced by multilevel movements [2, 6]. New studies based on real human mobility
19 data also provide evidence to support the argument that individual movements occur at different
20 levels [11, 12].

21 Another thing to consider is that the ways individuals interact with each other. Interactions
22 between individuals involve both within-patch interactions and between-patch interactions. It is
23 assumed that the contacts between individuals on each patch are frequent and hence random mix-
24 ing applies within the subpopulation. Between-patch interactions are of more interest and usually
25 modelled by two methods, depending on the frequency of movements. If the interaction between
26 two patches is dominated by frequent movements (e.g. people commuting to and from work), the
27 subpopulations are said to be interacting with each other in a way like particles randomly bumping
28 into each other. In other words, any infection occurring on one patch has the force of infection on
29 the susceptible individuals in the closely related patches [1, 13, 14]. The force of infection is defined
30 as the per capita rate that the infected individuals transmit the disease to susceptible individu-
31 als [15]. Alternatively, if the movements between two patches mainly take the form of migration,
32 it means that individuals migrate to the host population with the disease status they get from the
33 home patch first and then take part in the disease transmission process in the host patch [1, 9].
34 These two scenarios were studied separately in the past [1, 13]. In real populations, it is obvious
35 that both scenarios occur simultaneously.

36 Here we build a metapopulation model based on multilevel movements including both patch-
37 coupling and migration. At the lowest level, where the population movements between the patches
38 are most frequent, the patches are coupled by the force of infection; while patches with less
39 frequent movements in between are linked by migration. In this paper, these two kinds of patch
40 relationships are referred to as close-related patches and not close-related patches. Moreover, it
41 does not necessarily mean that well-connected patches are geographically close, in contrast to
42 previous work [2]. Human mobility tends to be more complex than animal migration or plant
43 dispersal and is not necessarily related to geographic distances [16, 17].

44 **2 The model**

45 The hierarchical system we set up to describe the metapopulation model consists of L levels of
46 movements. The number of patches at the same level is denoted by a fixed branching ratio B

47 for simple indexing. Therefore the total number of patches is B^L , denoted by n . We assume that
 48 the fewer the movements between two patches, the larger level difference (D) between them. The
 49 level difference is the number of levels to reach the common ancestor node in the hierarchy. The
 50 level difference between close-related patches, i.e. the first level when counting levels, is defined
 51 as 0. One possible system is illustrated in Figure 1 as an example. Individuals are assumed to be
 52 homogeneously mixed within each patch. All patches are assumed to have identical within-patch
 53 population dynamics and environmental conditions [8]. Person-to-person contact, which leads to
 54 disease transmission, takes place when individuals meet in one of the n patches. Patches interact
 55 with each other through either coupling or migration. Initially the total population is distributed
 56 evenly across all n patches and one infectious individual is introduced to the system. Individuals in
 57 each patch are classified in terms of their infection status: susceptible, infected or recovered, within
 58 which the numbers of individuals are denoted by S , I and R respectively. The susceptible class
 59 includes all healthy people with no immunity to the disease, the infected class includes people
 60 who have caught the disease. For simplicity, infected individuals are assumed to be infectious
 61 immediately. R denotes the recovered group, with lifelong immunity [13, 15]. We model a non-
 62 fatal, communicable disease, such as the common cold or influenza virus, spreading much faster
 63 than the natural demographic process. Therefore our basic framework is the simple SIR model
 64 (Equation 1) [15, 18]:

$$\begin{aligned}
 \frac{dS}{dt} &= -\beta IS \\
 \frac{dI}{dt} &= \beta IS - \gamma I \\
 \frac{dR}{dt} &= \gamma I
 \end{aligned} \tag{1}$$

65 where disease is transmitted through person-to-person contact which is modelled by the adequate
 66 contact rate for disease transmission (β) and recovery rate (γ). This is the normalised form,
 67 i.e. all the variables are proportions. It models the pure disease transmission process within a
 68 homogeneously mixed population without considering other effects, such as demographic effects,
 69 spatiotemporal effects and so forth. In our system, where the interactions between patches take
 70 two different forms, we need to consider both effects. The force of infection for the simple SIR
 71 model is βI . To generalise it to the single patch in our model, we need to consider that the force of
 72 infection on patch i is affected by the sum of the infection situations on the patches close-related
 73 to it, i.e. $\sum_j \beta_{j,i} I_j$, where $j \in J$, J : the set of indices of the patches close-related to patch i . In this
 74 model, we allow the adequate contact rate to vary between close-related patches [13] and therefore

75 we can examine the effects of different contacting rules on disease dynamics. The range of values
 76 of β is consistent with that for influenza [15].

77 The other process that changes the number of infected individuals in patch is migration. Both
 78 emigration and immigration are assumed to operate between two patches which are not close-
 79 related. The per capita migration rates of infected, susceptible and recovered groups in the whole
 80 system are denoted by θ , ϕ and ξ respectively. The immigration rate of susceptible individuals
 81 from another patch to patch i is calculated by a function $\theta_{ki} = \theta C e^{-CD}$, where $k \in K$, K : the set
 82 of indices of the patches linked to patch i by migration. The subscript ki indicates immigration
 83 and ik emigration. $C e^{-CD}$ is a normalised general exponential function. It is the simplest form
 84 for representing the mechanism that the migration rate decays as the level difference between
 85 two patches increases. C is a constant, which scales the function and D is the level difference
 86 (described above). Similarly, $\phi_{ki} = \phi C e^{-CD}$ and $\xi_{ki} = \xi C e^{-CD}$ describe the rates of movement for
 87 infected and recovered individuals respectively. Finally, all the immigrants from different patches
 88 are summed and all the emigrants to different patches are subtracted for each disease group to get
 89 the total proportion of immigrants and emigrants.

90 As we described above, because all the patches are homogeneous in population distributions,
 91 disease spreading behaviours and patterns of between-patch movements, we are able to express
 92 the population dynamics on an arbitrary patch i into a differential equation form (Equation 2):

$$\begin{aligned}
 \frac{dS_i}{dt} &= -\left(\sum_j \beta_{ji} I_j\right) S_i + \sum_k \theta_{ki} S_k - \sum_k \theta_{ik} S_i \\
 \frac{dI_i}{dt} &= \left(\sum_j \beta_{ji} I_j\right) S_i - \gamma I_i + \sum_k \phi_{ki} I_k - \sum_k \phi_{ik} I_i \\
 \frac{dR_i}{dt} &= \gamma I_i + \sum_k \xi_{ki} R_k - \sum_k \xi_{ik} R_i
 \end{aligned} \tag{2}$$

93 All migration parameters have very small values in this paper and therefore have little effect on
 94 the variability of local population dynamics during the simulation. All simulations are run until
 95 equilibrium is reached. Here we use two systems with the same number of patches in total: 1)
 96 branching ratio of four ($B = 4$) and level of three ($L = 3$); 2) branching ratio of two ($B = 2$) and
 97 level of six ($L = 6$).

98 3 Results

99 Figure 2 shows the time series of proportion of infected individuals for β being uniformly dis-
100 tributed and normally distributed. More fluctuations and different sizes and durations of the in-
101 fection changes are observed with the uniform distribution. It shows smaller but longer epidemics
102 in the uniform distribution based model than those when β is drawn from a truncated normal
103 distribution.

104 In previous work using hierarchical metapopulation models, contacts between patches are based
105 solely on migration behaviours [2, 6] and comparison results with and without patch-coupling is
106 shown in Figure 3. It clearly shows that patch-coupling accelerates the spread of the disease through
107 the system and leads to more cases, even with a smaller contact rate for disease transmission.

108 4 Discussion

109 Combining close-related patches and migration-related patches, we obtain behaviours not observed
110 in previous studies [2, 6]. A uniform distribution of β means that we have little prior knowledge of
111 the adequate contact rates on patches, so the random chosen value has equal opportunities to stay
112 at any point within the lower and upper bounds. We have 64 uniformly distributed random num-
113 bers and we expect strong stochasticity. The results illustrated in Figure 2 confirm this. On the
114 other hand, 64 normally distributed random numbers tend to surround the mean. Consequently
115 we observe some randomness but still see the three-level pattern. In conclusion, estimating the
116 adequate contact rates in real life is an important step towards choosing right models for predic-
117 tions.

118 It was shown by previous studies that patch-coupling is a quick way for the disease dynamics on
119 each patch to synchronise [13, 14], but observing the effects in a multilevel metapopulation model
120 was not realised. We obtained a larger epidemic with even smaller contact rates for transmission in
121 a model including patch-coupling. Therefore it demonstrates that epidemics are likely to be much
122 worse in a large population where movements are frequent between sub-populations. We suggest
123 that health authorities cannot ignore an infectious disease with low transmission rate that occurs
124 in a large population where people have more frequent short-trips between subpopulations.

125 We promote a model based on both frequent movements and long-lived travels and it shows
126 that differentiated contact rates make the disease dynamics more complicated but still tractable.
127 Since local information of contact rates are not usually collected [14], we expect that investigations

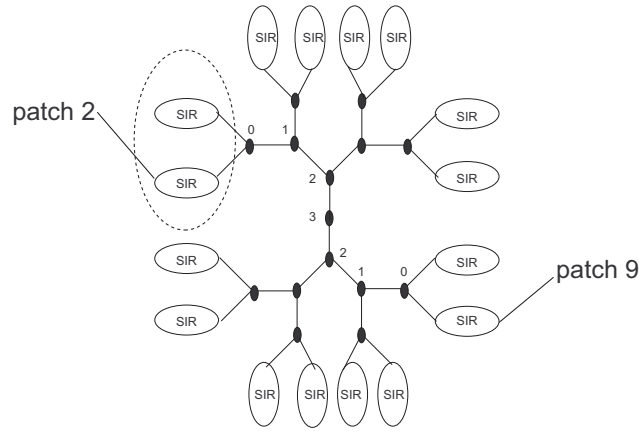


Fig. 1. One example of the multilevel system ($B = 2$, $L = 4$). The small ellipses represent the patches, the black nodes illustrate the different levels and the dashed ellipse represent one example of close-related patches. *SIR* means that the simple Susceptible-Infected-Recovered process applies within each patch. It also shows an example of calculating the value of D , the level difference between any two patches (see method for description). $D = 3$ for patch 2 and patch 9 (anticlockwise numbering) according to the levels they belong to (i.e. you have to move up three levels before these two patches share a common node).

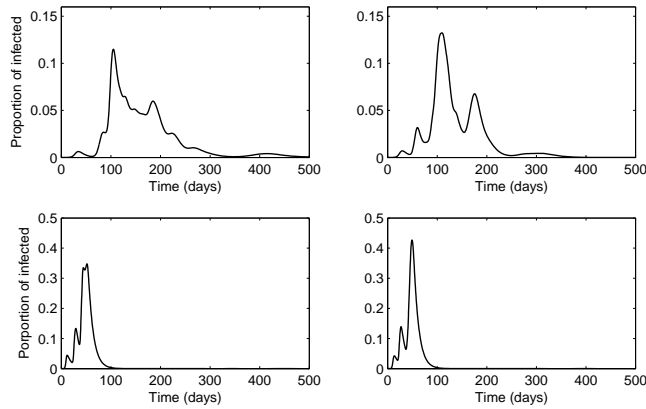


Fig. 2. The effects of two different distributions of β on disease spreading. $B = 4$, $L = 3$. (Top): two simulations based on a uniform distribution of β ($0.0 < \beta < 0.6$); (Bottom): two simulations based on a truncated normal distribution of β (mean = 0.3, standard deviation = 0.1, $0.0 < \beta < 0.6$). It shows that we get smaller but longer epidemic from the uniform distribution based model then those from the normal distribution. Moreover, the results from the uniform distribution are more stochastic.

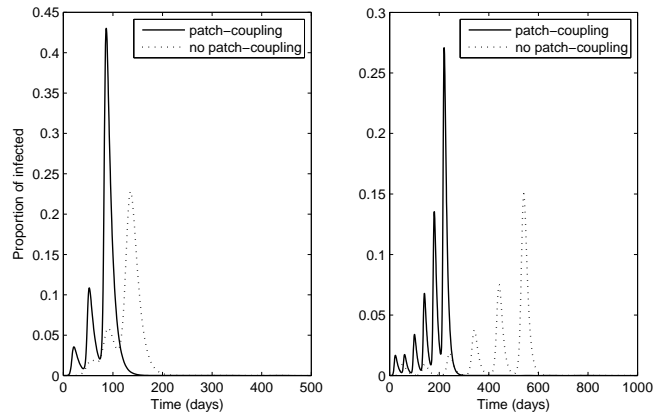


Fig. 3. Comparison between migration-based model and patch-coupling-migration-based model for two systems: $B = 4, L = 3$ (Left); $B = 2, L = 6$ (Right). For migration-based simulations (dashed line), $\beta = 0.3$ is used; whereas $0.1 < \beta_{ki} < 0.3$ is applied for patch-coupling-migration-based simulations (solid line), which means the adequate contact rate on average is smaller than three. It shows that even with a smaller contact rate, the size of epidemic is not reduced for patch-coupling-migration-based model. It also shows that the synchronisation of the system is more rapid in the patch-coupling-migration-based model.

128 on such data will be helpful both for validating the model and for facilitating better prediction of
 129 the spread of diseases through human populations.

130 5 Acknowledgements

131 We thank Graham R. Law and Kate E. Pickett for persistent support, Alun L. Lloyd, Roby
 132 Muhamad and Duncan J. Watts for answering questions. XW is funded by a studentship from the
 133 Department of Health Sciences at the University of York.

134 References

- 135 1. Lloyd, A.L., Jansen, V.A.A.: Spatiotemporal dynamics of epidemics: synchrony in metapopulation
 136 models. *Math Biosci* **188** (2004) 1–16
- 137 2. Watts, D.J., Muhamad, R., Medina, D.C., Dodds, P.S.: Multiscale, resurgent epidemics in a hierar-
 138 chical metapopulation model. *Proc Natl Acad Sci U S A* **102**(32) (Aug 2005) 11157–11162
- 139 3. Volz, E., Meyers, L.A.: Susceptible-infected-recovered epidemics in dynamic contact networks. *Proc*
 140 *Biol Sci* **274**(1628) (Dec 2007) 2925–2933
- 141 4. Gandon, S., Mackinnon, M., Nee, S., Read, A.: Imperfect vaccination: some epidemiological and
 142 evolutionary consequences. *Proc Biol Sci* **270**(1520) (Jun 2003) 1129–1136

- 143 5. Boots, M., Meador, M.: Local interactions select for lower pathogen infectivity. *Science* **315**(5816)
144 (Mar 2007) 1284–1286
- 145 6. Wang, X., Dytham, C., Law, G.R.: The effects of multilevel metapopulation structure and migration
146 kernels on disease spread. under review (August 2008)
- 147 7. Levins, R.: Some demographic and genetic consequences of environmental heterogeneity for biological
148 control. *Bull. Entomolog. Soc. America* **15** (1969) 237–240
- 149 8. Hess, G.: Disease in metapopulation models: Implications for conservation. *Ecology* **77**(5) (1996)
150 1617–1632
- 151 9. Jansen, V.A., Lloyd, A.L.: Local stability analysis of spatially homogeneous solutions of multi-patch
152 systems. *J Math Biol* **41**(3) (Sep 2000) 232–252
- 153 10. Hufnagel, L., Brockmann, D., Geisel, T.: Forecast and control of epidemics in a globalized world. *Proc*
154 *Natl Acad Sci U S A* **101**(42) (Oct 2004) 15124–15129
- 155 11. Brockmann, D., Hufnagel, L., Geisel, T.: The scaling laws of human travel. *Nature* **439**(7075) (Jan
156 2006) 462–465
- 157 12. González, M.C., Hidalgo, C.A., Barabási, A.: Understanding individual human mobility patterns.
158 *Nature* **453**(7196) (Jun 2008) 779–782
- 159 13. Lloyd, A.L., May, R.M.: Spatial heterogeneity in epidemic models. *J Theor Biol* **179**(1) (Mar 1996)
160 1–11
- 161 14. Keeling, M.J., Rohani, P.: Estimating spatial coupling in epidemiological systems: a mechanistic
162 approach. *Ecology Letters* **5** (2002) 20–29
- 163 15. Anderson, R.M., May, R.M.: *Infectious diseases of humans : dynamics and control*. Oxford University
164 Press (1991)
- 165 16. Brown, D.H., Bolker, B.M.: The effects of disease dispersal and host clustering on the epidemic
166 threshold in plants. *Bull Math Biol* **66**(2) (Mar 2004) 341–371
- 167 17. Colizza, V., Barrat, A., Barthélemy, M., Vespignani, A.: The role of the airline transportation network
168 in the prediction and predictability of global epidemics. *Proc Natl Acad Sci U S A* **103**(7) (Feb 2006)
169 2015–2020
- 170 18. Kermack, W.O., McKendrick, A.G.: A contribution to the mathematical theory of epidemics. *Proc.*
171 *Royal Soc. London* **115**(1-2) (1927) 700–721